

A Novel Shunt Active Power Filter Topology for Driving huge Power Drive Applications

A. Bhakthavachala^a, S. Tara kalyani^b, K. Anuradha^c, B.V. Naveen Teja^d

^aResearch Scholar, department of EEE, Jawaharlal Nehru Technological University, Hyderabad, India.

^bProfessor & Head, EEE, Jawaharlal Nehru Technological University, Hyderabad, India-500085.

^cProfessor & Head, EEE, VNR Vignana Jyothi Institute of Technology, Hyderabad, India-500085.

^dM.Tech, PG student, PBR Visvodaya institute of technology and science, kavali-524201.

Abstract—In high-power adjustable-speed motor drives, such as those used in electric ship propulsion systems, active filters provide a viable solution to mitigating harmonic related issues caused by diode or thyristor rectifier front-ends. To handle the large compensation currents and provide better thermal management, two or more paralleled semiconductor switching devices can be used. In this paper, a novel topology is proposed where two active filter inverters are connected with tapped reactors to share the compensation currents. The proposed active filter topology can also produce seven voltage levels, which significantly reduces the switching current ripple and the size of passive components. Based on the joint redundant state selection strategy, a current balancing algorithm is proposed to keep the reactor magnetizing current to a minimum. It is shown through simulation that the proposed active filter can achieve high overall system performance. The system is also implemented on a real-time digital simulator to further verify its effectiveness. Index Terms—Active filters, harmonic analysis, power conversion, power electronics.

I. INTRODUCTION

Adjustable-speed motor drives (ASDs) have found extensive application in a variety of high-power systems. One example is the electric propulsion system used in modern naval ships, the power ratings of which can be tens of megawatts. Typically, the front-ends of such ASDs employ a diode or a thyristor rectifier. In spite of their simple control and robust operation, these devices can generate voltage and current harmonics that might affect the operation of other devices in the same acsystem. Conventionally, passive LC filters are used to mitigate harmonic-related problems. However, due to their large size and inflexibility, passive filters are gradually being replaced by active filters that utilize power electronic inverters to provide compensation for harmonics [1]. Among various active filter

configurations, the shunt active filter systems have a number of advantages and constitute the optimal harmonic filtering solution for ASD rectifier front-ends [2]. In general, the ratings of shunt active filters are based on the rms compensating current and the rms filter terminal voltage. For high-power applications such as ship propulsion systems, the large compensation current often requires parallel operation of two or more switching devices or active filters. In recent years, multilevel converters have shown some significant advantages over traditional two-level converters [3]–[5], especially for high-power and high-voltage applications. In addition to their superior output voltage quality, they can also reduce voltage stress across switching devices. Since the output voltages have multiple levels, lower dv/dt is achieved, which greatly alleviates electromagnetic interference problems due to high-frequency switching. Over the years, most research work has focused on converters with three to five voltage levels [4], [5], although topologies with very high number of voltage levels were also proposed [6]. In general, the more voltage levels a converter has, the less harmonic and better power quality it provides. However, the increase in converter complexity and number of switching devices is a major concern for a multilevel converter. It has been shown that although more voltage levels generally mean lower total harmonic distortion (THD), the gain in THD is marginal for converters with more than seven levels [7]. This paper presents a shunt active filter configuration that uses tapped reactors for harmonic current sharing. It reduces current stress of the switching devices by distributing the compensation current between two parallel legs of an H-bridge topology. It also reduces voltage stress across the switches by utilizing a conventional three-level flying capacitor topology. Overall, the configuration is capable of producing seven distinct voltage levels, and thus, greatly reduces switching ripple in the compensating currents. The concept of the configuration was

introduced in a previous conference publication [8]. Herein, more detail of the topology and control are presented. Additional simulation studies are also carried out as well as corresponding studies using a real-time digital simulator (RTDS). The studies herein are also conducted on a full motor drive system, whereas in the previous work, the system was supplying a resistive load. The rest of this paper is organized as follows. The active filter topology is briefly described in Section II. The control algorithm of the active filter is discussed in Section III. Simulation results are presented in Section IV to evaluate the proposed configuration and control. In addition, the system is implemented on RTDS hardware to further validate the proposed active filter, and the results are also presented in Section V. Finally, the conclusions are given in Section VI.

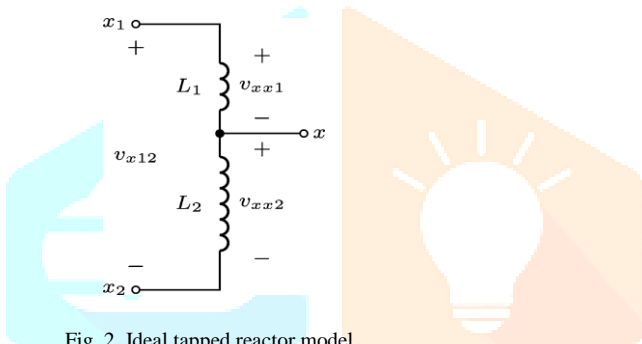
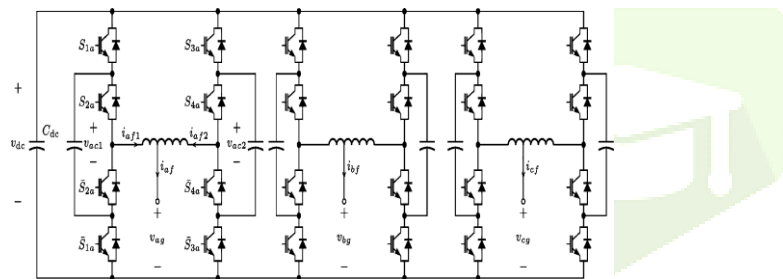


Fig. 2. Ideal tapped reactor model.



II. ACTIVE FILTER TOPOLOGY

The proposed active filter topology is shown in Fig. 1. It consists of an H-bridge configuration made from three-level flying capacitor branches. Essentially, it is a voltage-source inverter (VSI) with capacitive energy storage (C_{dc}) shared by all three phases. A total of eight switching devices are used in each phase. A tapped reactor is used to connect the two legs of the H-bridge. Typically, the reactor is wound to be centre tapped, making the output line-to-ground voltages (v_{ag} for example) the average of the voltages from each

Fig. 1. Proposed seven-level active filter topology.

side of the H-bridge. Then, the line-to-ground voltages will have five distinct voltage levels [9]–[12]. However, with this topology, the tap is set at 1/3. This results in

seven distinct output voltages, and therefore, improves the power quality. The switching operation is described next, wherein all seven levels are clearly illustrated.

A. Tapped Reactor Model

Unlike the center-tapped interphase reactor [9]–[12], the reactor in the proposed topology has a tap terminal at its one-third position, as shown in Fig. 2. For the convenience of analysis, the reactor can be divided into two parts. In Fig. 2, part one, denoted as L₁, consists of the portion from terminal x₁ to the tap and has a number of turns N₁ = N; part two, denoted as L₂, consists of the portion from the tap to terminal x₂ and has a number of turns N₂ = 2N. Terminals x₁ and x₂ are defined as the input terminals while the tap terminal is defined as the output terminal x. To derive the relationship between the input voltages and the output voltage, an ideal model of the tapped reactor is considered first in which there are no losses and no leakage flux. The following assumptions are made.

TABLE I
ACTIVE FILTER LINE-TO-GROUND VOLTAGES

s_a	v_{a1}	v_{a2}	v_{ag}
0	0	0	0
1	0	$v_{dc}/2$	$v_{dc}/6$
2	$v_{dc}/2$	0	$v_{dc}/3$
2'	0	v_{dc}	$v_{dc}/3$
3	$v_{dc}/2$	$v_{dc}/2$	$v_{dc}/2$
4	$v_{dc}/2$	v_{dc}	$2v_{dc}/3$
4'	v_{dc}	0	$2v_{dc}/3$
5	v_{dc}	$v_{dc}/2$	$5v_{dc}/6$
6	v_{dc}	v_{dc}	v_{dc}

- 1) The core of the reactor is highly permeable in a sense that it requires vanishingly small magnetomotive force to set up the flux.
- 2) The core does not exhibit any eddy current or hysteresis loss.
- 3) All the flux is confined in the core, so there is no leakage flux.
- 4) The resistance of the reactor is negligible. Suppose that voltages v_{x1} and v_{x2}, with respect to a common ground, are applied to the input terminals x₁ and x₂, respectively. For this ideal model, it is straightforward to determine the voltage between the output terminal x and terminal x₂

$$V_{xx2} = \left\{ \frac{N_2}{(N_1+N_2)} \right\} (V_{x1} - V_{x2}) = \frac{2}{3} (V_{x1} - V_{x2}) \text{-----(1)}$$

The voltage at the output terminal with respect to the common ground is therefore

$$V_{xg} = V_{xx2} + V_{x2} = \frac{2}{3}V_{x1} + \frac{1}{3}V_{x2} \dots \dots (2)$$

In the general analysis presented earlier, x represents a phase, and the phase may be a, b, or c. Each leg of the H-bridge has a voltage-clamping capacitor, and the voltages at the two input terminals of the reactor can be 0, vdc/2, or vdc, where vdc is the nominal voltage of the capacitor Cdc, as shown in Fig. 1. For each phase, there are nine different switching states, corresponding to nine terminal voltage combinations. These combinations can produce a line-to-ground voltage at the output terminal that has seven distinct voltage levels. For phase a, these states are detailed in Table I. In Table I, sa is the switching state that is defined as being 0 for the lowest possible line-to-ground voltage. The voltages va1 and va2 are the line-to-ground voltages applied to the left and right side of the reactor in Fig. 1, respectively. The voltage vag is as defined in Fig. 1 and calculated using (2). Note that there are two redundant states 2 and 4 that produce the same voltage as states 2 and 4, respectively. However, these are not desirable, and will be ignored, because the voltages applied across the reactor are twice as high as the other states. The output current for each phase is split between the two legs of the H-bridge structure. Ideally, two-thirds of the current will come from x1 and one-third from x2 so that the magnetizing current is zero. The control given later discusses the regulation of the reactor currents so as to minimize the magnetizing current.

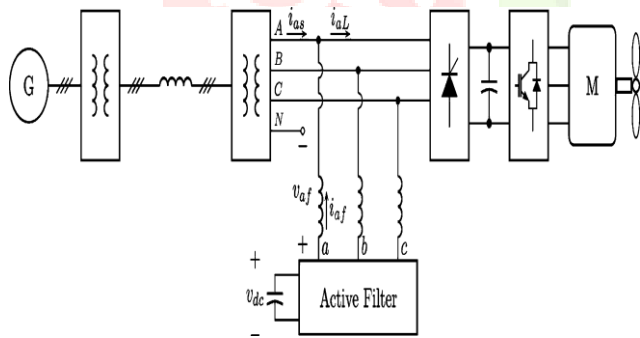


Fig. 3. Active filter connection to a shipboard power system.

B. Active Filter Interface

As shown in Fig. 3, the active filter is connected to the power system via a three-phase inductor Lf. The filtering function is achieved by injecting a compensating harmonic current into the point of common coupling of the utility-load interface, which in this case is the secondary side of the rectifier load transformer. The reference harmonic currents are extracted from the load currents so that the sum of the load currents and the injection currents has a THD that meets required

specifications. The seven-level inverter can produce an output voltage that contains much less switching frequency ripple than a conventional twolevel inverter; thus, the generated injection currents are smoother and the coupling inductor can be reduced. According to the inverter equations, the line-to-neutral voltage vaf depicted in Fig. 3 can be related to the inverter line-to-ground voltages by [13]

$$V_{af} = \frac{2}{3}v_{ag} - \frac{1}{3}v_{bg} - \frac{1}{3}v_{cg} \dots \dots (3)$$

Having established the model for the proposed active filter, the following section describes the details of the control.

III. ACTIVE FILTER CONTROL

To effectively compensate the load harmonic currents, the active filter controller should be designed to meet the following three goals:

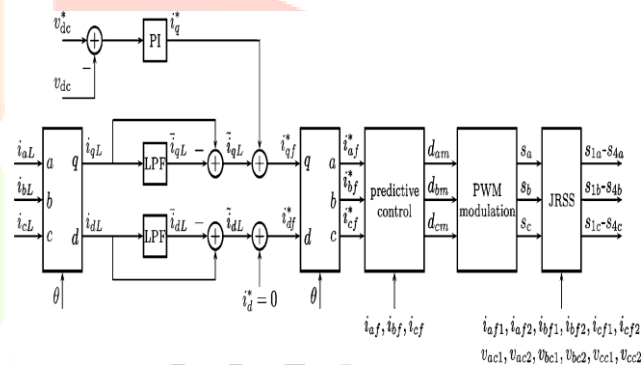


Fig. 4. Active filter control diagram.

- 1) extract and inject load harmonic currents;
- 2) maintain a constant dc capacitor voltage;
- 3) avoid generating / absorbing reactivepower with fundamental frequency components.

A. Harmonic Current Extraction

For diode or thyristor rectifier loads, the most common harmonic currents are of the 5th, 7th, 11th, and 13th order. Although a high-pass filter can be used to extract these components directly from the line currents, it is not feasible to obtain high attenuation at the fundamental frequency due to the high current amplitude. The synchronous q-d reference frame controller developed for shunt active filter systems is used to generate the reference compensating current [2]. As shown in Fig. 4, the measured load phase currents (iaL, ibL, and icL) are

first transformed into the synchronous reference frame to obtain i_{qL} and i_{dL} . The synchronous reference frame phase angle can be obtained by processing the measured system voltage with a phase-locked loop circuit or algorithm. Low-pass filters are then used to extract the dc components, which correspond to the fundamental frequency components of the load currents. The dc component is removed by a simple subtraction of the filtered components (\bar{i}_{qL} and \bar{i}_{dL}) and the transformed components (i_{qL} and i_{dL}).

B. DC Capacitor Voltage Control

For the active filter to operate effectively, it is important to maintain the dc capacitor voltage at a constant value. Since the active filter topology is essentially identical to that of an active filter, similar control strategies for the active rectifier are applicable. The dc capacitor voltage is directly affected by the real power transferred across the active filter. To keep the voltage constant, ideally, no real power should be transferred. However, due to losses in switching devices and other components, a small amount of real power is needed. In the synchronous reference frame with the q-axis aligned with the voltage at the point of common coupling, the real power transferred can be expressed as

$$P = \frac{3}{2} v_{qs} i_{qf} \quad \text{--- (4)}$$

which means that by adjusting the q-axis filter current, the real power can be effectively controlled. The capacitor voltage regulation is then handled by a simple proportional-integral (PI) control adding to the q-axis filter current, as shown in Fig. 4.

C. Reactive Power Control

In most cases, a unity power factor for fundamental frequency components is required at the active filter terminals. Since the reactive power can be expressed as

$$Q = \frac{3}{2} v_{qs} i_{df} \quad \text{--- (5)}$$

this goal can be achieved by keeping the average d-axis current at zero, as shown in Fig. 4. The combined control of dc capacitor voltage and reactive power uniquely determines the fundamental frequency component of the active filter output current. This current is then superimposed onto the commanded harmonic currents, and the commanded filter currents i_{af}^* , i_{bf}^* , and i_{cf}^* are

obtained by the reverse transformation, as shown in Fig. 4

D. Harmonic Current Regulator

A current regulator is needed to generate the commanded compensation current. Generally, a hysteresis control provides fast response and is suitable for nonsinusoidal current tracking. However, it suffers from some serious disadvantages such as variable switching frequency and phase interaction problems [1]. In addition, to fully take advantage of the benefits of a multilevel converter, a current regulator that uses a voltage-source pulsewidth modulation (PWM) is desirable. Several frequency-selective harmonic current regulators were proposed in [14]–[17] that achieve zero steady-state error for the dominant harmonics. Nonetheless, they all have to target specific frequencies and require a significant amount of computation time. In this paper, a predictive current regulator is implemented to track the harmonic currents, which has the advantages of simple structure and less computational requirement. Given the measured system voltages and filter inductor currents, the required phase a filter voltage can be calculated based on the known value of the filter inductance

$$v_{af}^* = v_{as}^{\wedge} + \frac{(i_{af}^* - i_{af})L_f}{\Delta t} \quad \text{--- (6)}$$

Where Δt is the controller switching period, v_{as}^{\wedge} is the predicted source voltage and can be calculated through linear extrapolation

$$v_{as}^{\wedge} = v_{as} + 1.5\Delta t[v_{as}(t) - v_{as}(t - \Delta t)] \quad \text{--- (7)}$$

and i_{afis}^{\wedge} is the predicted reference harmonic current

$$i_{af}^{\wedge*} = i_{af}^*(t) + 2\Delta t[i_{af}^*(t) - i_{af}^*(t - \Delta t)] \quad \text{--- (8)}$$

For accurate current tracking, the prediction takes into account the controller delay due to data acquisition and calculation. Better performance has been achieved when a second-order prediction method is used. As can be seen, the predictive control effectively turns the commanded currents into commanded voltages suitable for a voltage-source modulator. These commanded voltages are then expressed as PWM duty cycles by normalizing them to the dc voltage and giving them an appropriate range. For phase a, the duty cycle can be expressed as

$$d_{am} = \left(\frac{v_{af}^*}{v_{dc}} + 0.5 \right) (n - 1) \dots \dots \dots (9)$$

Where n is the number of voltage levels, which for this topology is n = 7. Similar expressions can be written for phase b and phase c. The predictive control is shown in Fig. 4 having outputs to the PWM modulator, which is described next.

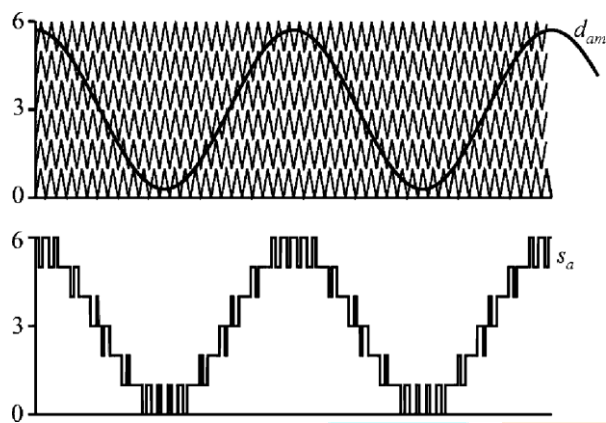


Fig. 5. Seven-level voltage-source modulation

E. Multilevel Voltage-Source Modulation

The seven-level voltage-source modulation is accomplished by comparing the duty cycles with a set of six carrier waveforms. This is illustrated for phase a in Fig. 5. The resulting switching state sa is the number of triangle waveforms that the duty cycle is greater than. Therefore, the switching state has a range of 0–6, and this is in agreement with Table I.

F. Capacitor Voltage Balancing

After carrying out the modulation, the switching states for each phase need to be broken out into transistor signals. In order to have the correct voltage levels, the flying capacitors must remain charged at exactly vdc/2. This can easily be assured using the redundancy of the inverter legs.

For each leg of the H-bridge structure, there are four switches and a total of four switching states. Two of the switching states can produce the same vdc/2 output, which provides great flexibility for capacitor charging and discharging. Table II shows the relationship between switching states, output current direction, and capacitor charging/discharging, where the left leg of phase a bridge is used as an example. The designations of the variables can be found in Fig. 1. The + and – signs for the output current denote the polarity of the current. The charging status of the flying capacitor can be + (charging), – (discharging), or 0 (neither charging nor discharging). It

can be seen that for state (s1a , s2a) = (0, 0) and (1, 1), output current does not flow through the flying capacitor; therefore, the capacitor voltage does not change. The two redundant states (1, 0) and (0, 1) produce the same output voltage vdc/2. Both can be used to charge or discharge the capacitor, depending on the direction of output current. For example, if the output current is positive, one can pick (1, 0) to charge the flying capacitor, or pick (0, 1) to discharge it. This simple decision is made instantaneously online depending on the state of charge of the flying capacitors.

TABLE II
FLYING CAPACITOR VOLTAGE BALANCING

s _{1a}	s _{2a}	v _{a1}	i _{af1}	Charging
0	0	0	+	0
0	0	0	–	0
1	1	v _{dc}	+	0
1	1	v _{dc}	+	0
0	1	v _{dc} /2	+	–
0	1	v _{dc} /2	–	+
1	0	v _{dc} /2	+	+
1	0	v _{dc} /2	–	–

G. Magnetizing Current Minimization

The current through the reactor consists of two components. One is the compensating current that flows out of the tap terminal and is shared by the two parts of the reactor. The other is the magnetizing current that is generated when an average voltage is applied across the reactor input terminals. The magnetizing current does not contribute to the filtering function and should be minimized to reduce current ratings of the switching devices and avoid reactor saturation. Ideally, the magnetizing current has a zero average component. In practice, however, the magnetization current tends to drift away from zero if uncontrolled because of the differences in component parameters and controller errors. Therefore, it is necessary to monitor and control the magnetizing currents of the reactors in each phase so that their values are within a limited range. Let the magnetizing current in phase a be iam, then the following relationship holds if two-thirds of the filter current is to come from the left side of the reactor

$$i_{am} = 2i_{af2} - i_{af1} \dots \dots \dots (10)$$

The magnetizing current can be minimized by balancing the average voltage applied across the tapped reactor.

Among the seven switching states in Table I, the states ($V_{a1}= 0, V_{a2}= 0$), ($V_{a1}= V_{dc}/2, V_{a2}=V_{dc}/2$), and ($V_{a1} = V_{dc}, V_{a2}= V_{dc}$) have no effect on the magnetizing current, while the other four states can either increase or decrease the magnetizing current. Since states 2 and 4 are not used, there is no usable per-phase redundant state. Thus, the magnetizing current of each phase cannot be adjusted independently. In this paper, a technique similar to the joint-phase redundant states selection (JRSS) method proposed in [7] is used to minimize the magnetizing currents. The concept behind JRSS is that for a three-phase inverter, the line-to-ground voltages of all phases may be changed simultaneously without affecting the load voltages since the terms that are common in all phases will cancel when looking at the line-to-line voltages or line-to-neutral voltages, as seen by (3). The magnetizing current minimization procedure is as follows. At the beginning of each switching period, the magnetizing current for each phase is calculated. Suppose the commanded voltage levels are s_i , where $i = a, b, c$, and $0 \leq s_i \leq 6$. The number of available joint redundant states is

$$k = \min(s_i) + 6 - \max(s_i) \quad (11)$$

Each redundant state specifies the three-phase active filter voltage levels. Based on Table I, the voltage applied across the reactor for each phase and whether the magnetizing current increases, decreases, or does not change can be determined. If the magnetizing inductance L_m is known, the change in the current (for phase a) can be calculated as

$$\Delta i_{am} = \frac{v_{a1} - v_{a2}}{L_m} \Delta t \quad (12)$$

where V_{a1} and V_{a2} are voltages at the two terminals of the reactor and Δt is the duration of the state. The change in current as predicted by (12) is used along with the measured value of magnetizing current to predict the value of magnetizing current at the next controller time step. The switching state that results in the minimum predicted magnetizing current for all three phases is selected. The calculation block representing the JRSS control is shown at the output of the modulator in Fig. 4. The inputs are taken as switching states from the modulator, which represent commanded voltage levels. The JRSS block performs the calculations as described earlier and determines a new set of states that will lead to minimized magnetization currents. As a practical matter, the flying capacitor voltage regulation is also performed

in this block. The outputs are transistor signals, as labeled in Fig. 1. It should be pointed out that this block also reads in analog information of the flying capacitor voltages and the reactor currents to perform this regulation. Therefore, it is a feedback control that compensates to minimize magnetization current.

IV. SIMULATION RESULTS

Numerical simulations have been conducted in the Advanced Continuous Simulation Language (ACSL) to validate the proposed topology.

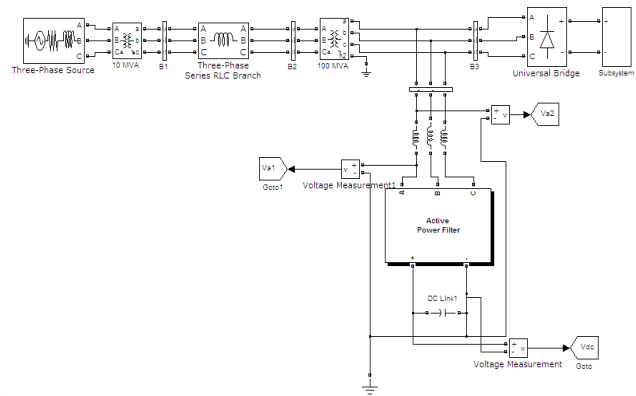
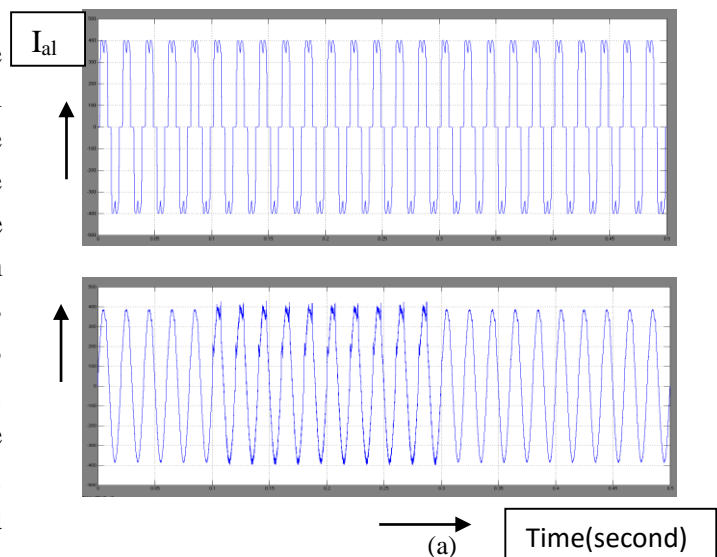


Fig. Simulation block diagram

The example naval ship power system has a rated line-to-line voltage of 4.16 kV and a three-phase six-pulse diode rectifier. A three-phase PWM inverter is connected to the rectifier dc bus, and supplies power to a permanent-magnet synchronous motor load. The rated dc capacitor voltage of the active filter is 6800 V. The three-phase tapped reactor has a leakage inductance of $L1 = 50 \mu H$, winding resistance $r = 0.1 \Omega$, and mutual inductance $LM = 1 H$. The active filter interface inductance is $Lf = 0.1 mH$.



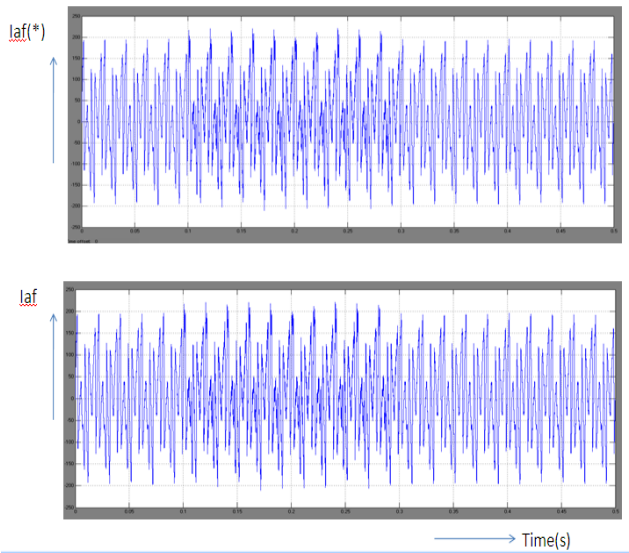


Fig. 6. Active filter detailed simulation results.

Fig. 6 shows the phase a operation of the active filter with a rectifier load. As can be seen, the load current i_{aL} contains a significant amount of harmonics. The active filter produces multilevel voltages that generate a current i_{aL}^* to cancel the harmonic contents. The compensated source current contains much less harmonics than i_{aL} .

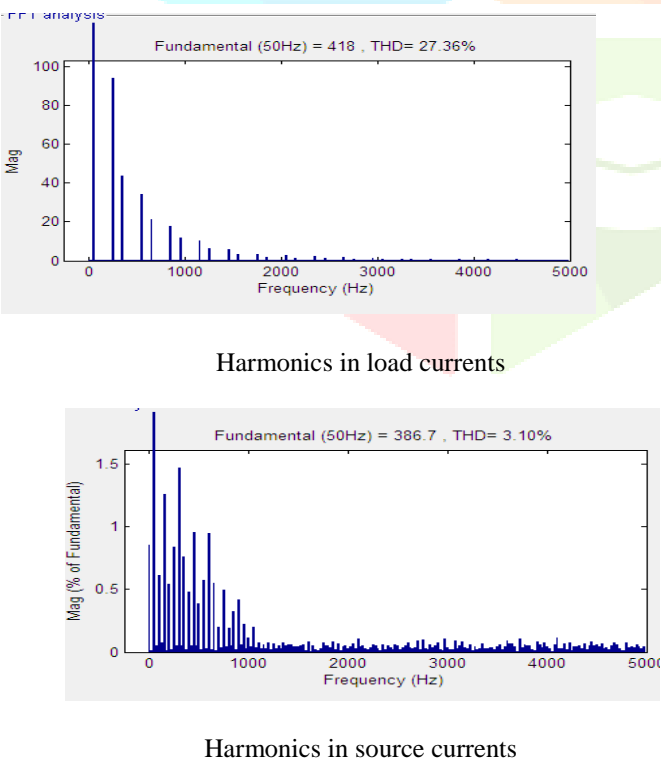
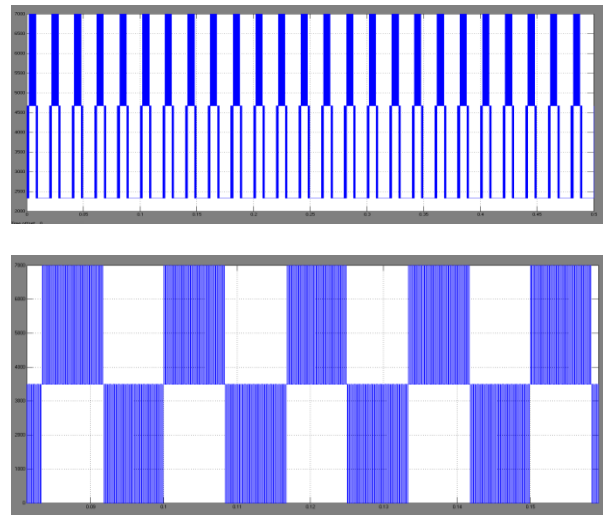


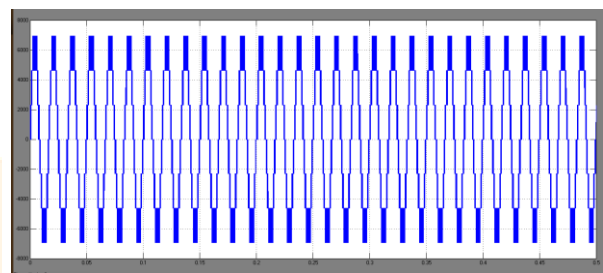
Fig. 7. Harmonic magnitude in load and source currents.

The magnitudes of the harmonic spectrum of the load and source currents are shown in Fig. 7. The THD of the load current is 25.1%, which is reduced to about 4.4% in the compensated source current. The source current still contains a certain amount of higher frequency

components. However, they are generally not a concern and can easily be removed by passive filters.



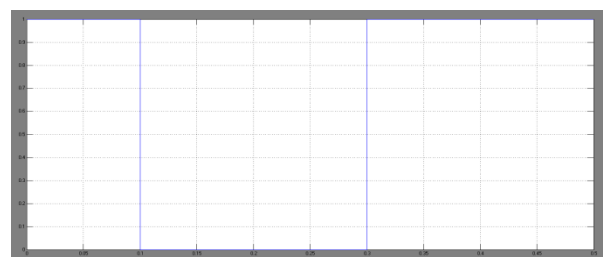
(a)



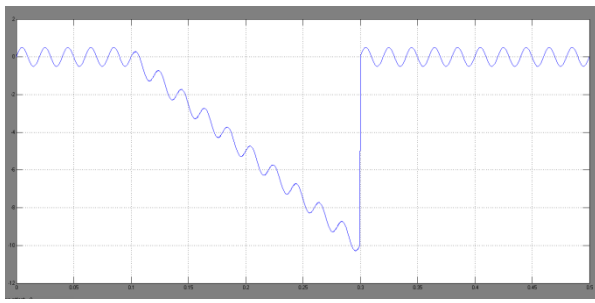
(b)

Fig. 8. Reactor terminal and output voltages.

To illustrate the generation of seven voltage levels, Fig. 8(a) shows the phase a line-to-dc-ground voltages applied at each end of the tapped reactor. These two voltages are produced by the flying capacitor legs and have three levels. The phase a converter-side line-to-neutral output voltage v_{af} from the ACSL simulation is shown in Fig. 8(b). Multiple voltage levels give the voltage a smooth shape that reduces injection current ripple. Also shown in Fig. 8(b) is the reactor output terminal to dc ground voltage v_{ag} , which has seven distinct levels. Note that because of joint redundant state selection, common-mode components are added to the line-to-ground voltages, which cause the irregular shape of v_{ag} .



(a)



(b)

Fig. 9. Magnetizing current with and without the balancing algorithm.

The effectiveness of the magnetizing current control is tested in simulation and illustrated in Fig. 9. The top part of Fig. 9 shows whether the JRSS current balancing algorithm is turned on or off, and the bottom part shows the magnetizing current in phase a. Initially, the balancing is ON, and it can be seen that the magnetizing current is kept within a small range with a very low dc component. At time $t = 0.1$ s, the balancing algorithm is turned off, and the magnetizing current drifts away from zero and keeps decreasing. In practice, a large magnetizing current can cause the iron core to saturate and eventually damage the reactor and switching devices. When the balancing method is turned on again, the magnetizing current returns to its minimum value.

VI. CONCLUSION

A new type of power converter has been introduced in this paper. The converter is based on parallel connection of phase legs through an interphase reactor. However, the reactor has an off-centre tap at one-third resulting in an increased number of voltage levels. Specifically, two three-level flying capacitor phase legs are paralleled in this way to form a seven-level power converter. The converter is utilized in an active filter application. The details of the high-level control as well as the switching control have been presented. The control ensures reactor current sharing as well as flying capacitor voltage balance. The proposed active filter has been validated for a naval ship board power system using detailed simulation and RTDS hardware.

REFERENCES

[1] B. Singh, K. Al-Haddad, and A. Chandra, "A review of active filters for power quality improvement," *IEEE Trans. Ind. Electron.*, vol. 46, no. 5, pp. 960–971, Oct. 1999.

[2] S. Bhattacharya, T. M. Frank, D. M. Divan, and B. Banerjee, "Active filter system implementation," *IEEE Ind. Appl. Mag.*, vol. 4, no. 5, pp. 47–63, Sep. 1998.

[3] Z. Du, L. M. Tolbert, and J. N. Chiasson, "Active harmonic elimination for multilevel converters," *IEEE Trans. Power Electron.*, vol. 21, no. 2, pp. 459–469, Mar. 2006.

[4] M. E. Ortuzar, R. E. Carmi, J. W. Dixon, and L. Moran, "Voltage-source active power filter based on multilevel converter and ultracapacitor DC link," *IEEE Trans. Ind. Electron.*, vol. 53, no. 2, pp. 477–485, Apr. 2006.

[5] B. R. Lin and T. Y. Yang, "Analysis and implementation of a three-level active filter with a reduced number of power semiconductors," *Proc. Inst. Electr. Eng. Electr. Power Appl.*, vol. 152, no. 5, pp. 1055–1064, Sep. 2005.

[6] M. Glinka, "Prototype of multiphase modular-multilevel-converter with 2MW power rating and 17-level-output-voltage," in *Proc. IEEE Power Electron. Spec. Conf.*, 2004, vol. 4, pp. 2572–2576.

[7] J. Huang and K. A. Corzine, "Extended operation of flying capacitor multilevel inverters," *IEEE Trans. Power Electron.*, vol. 21, no. 1, pp. 140–147, Jan. 2006.

[8] P. Xiao, K. A. Corzine, and G. K. Venayagamoorthy, "A novel sevenlevel shunt active filter for high-power drive systems," in *Proc. IEEE Ind. Electron. Soc. Conf.*, Paris, France, Nov. 2006, pp. 2262–2267.

[9] F. Ueda, K. Matsui, M. Asao, and K. Tsuboi, "Parallel-connections of pulsewidth modulated inverters using current sharing reactors," *IEEE Trans. Power Electron.*, vol. 10, no. 6, pp. 673–679, Nov. 1995.

[10] H. Mori, K. Matsui, K. Kondo, I. Yamamoto, and M. Hasegawa, "Parallelconnected five-level PWM inverters," *IEEE Trans. Power Electron.*, vol. 18, no. 1, pp. 173–179, Jan. 2003.

[11] K. Matsui, Y. Kawata, and F. Ueda, "Application of parallel connected NPC-PWM inverters with multilevel modulation for AC motor drive," *IEEE Trans. Power Electron.*, vol. 15, no. 5, pp. 901–907, Sep. 2000.

[12] S. Ogasawara, J. Takagaki, H. Akagi, and A. Nabae, "A novel control scheme of a parallel current-controlled PWM inverter," *IEEE Trans. Ind. Appl.*, vol. 28, no. 5, pp. 1023–1030, Sep. 1992.

[13] P. C. Krause, O. Wasynczuk, and S. D. Sudhoff, *Analysis of Electric Machinery and Drive Systems*, 2nd ed. New York: Wiley–IEEE Press, Feb. 2002.

[14] C. D. Schauder and S. A. Moran, "Multiple reference frame controller for active power filters and power line conditioners," U.S. Patent 5 309 353, May 1994.

[15] S. J. Lee and S. K. Sul, "A harmonic reference frame based current controller for active filter," in *Proc. IEEE Appl. Power Electron. Conf.*, New Orleans, LA, Feb. 2000, vol. 2, pp. 1073–1078.

[16] X. Yuan, W. Merk, H. Stemmler, and J. Allmeling, "Stationary-frame generalized integrators for current control of active power filters with zero steady-state error for current harmonics of concern under unbalanced and distorted operating conditions," *IEEE Trans. Ind. Appl.*, vol. 38, no. 2, pp. 523–532, Mar./Apr. 2002.

[17] R. I. Bojoi, G. Griva, V. Bostan, M. Guerriero, F. Farina, and F. Profumo, "Current control strategy for power conditioners using

sinusoidal signal integrators in synchronous reference frame," IEEE Trans. Power Electron., vol. 20, no. 6, pp. 1402–1412, Nov. 2005.



A. Bhaktha vachala received B.Tech. Degree from JNTU, Hyderabad in the year 2003, and M.Tech. degree from the same university in 2008. He is currently perusing Ph.D from JNTU Hyderabad. He has been working in the area of Electric Vehicle Applications in transportation systems from last five years. He has been with the department of Electrical and Electronics Engineering, PBR VITS, Kavali affiliated by JNTU Anantapur since 2007, where he is currently an Associate Professor. His research interests include several areas of power electronics and electric vehicle applications of power electronics. And he is the life member of ISTE.



Dr. S. Tara Kalyani received the B.Sc., degree in Electrical Engineering from Osmani University Hyderabad India in 1995, M.Sc. degree in the EEE from JNTU Hyderabad India in 1998. And also Ph.D., degree in Electrical Engineering from the Jawaharlal Nehru Technological University, Hyderabad, India in 2008. She is currently with the department of EEE in the JNTU, Hyderabad India, as a professor and head of the department. Her research interest includes Power Electronics, Control Systems, Fundamentals of Electrical Engineering, Energy Systems, Power Systems. She is a life member of Indian Society for Technical Education.



Dr. K. Anuradha received the B.E., degree in EE from Andhra University, Vizag, India; and the M.E. degree in electrical engineering from Osmania University, Hyderabad, India. And also Ph.D. degree in EE from Osmania University, Hyderabad, India, in 2011. She is currently with the Department of Electrical and Electronics Engineering in the VNR Vignana Jyothi Institute of Engineering & Technology Hyderabad, India, as a Professor and Head of the department. Her research interest includes Power Electronics and Drives. She is a life member of ISTE. She completed so many research projects from AICTE and UGC as a Principle Coordinator.



B. Venkata Naveen Teja received the B.E., degree in Electrical and Electronics Engineering from Jawaharlal Nehru Technological University, Anantapur, India. Now he is pursuing the M.E. degree in electrical engineering PBR Visvodaya Institute of Technology and Science, kavali affiliated with Jawaharlal Nehru Technological University, Anantapur.

